

# The Non–Mesonic Weak Decay of Double– $\Lambda$ Hypernuclei: A Microscopic Approach

E. Bauer<sup>1</sup>, G. Garbarino<sup>2</sup> and C. A. Rodríguez Peña<sup>3</sup>

<sup>1</sup>*Facultad de Ciencias Astronómicas y Geofísicas,  
Universidad Nacional de La Plata and IFLP,  
CONICET C. C. 67, 1900 La Plata, Argentina*

<sup>2</sup>*IIS G. Peano, I-10125 Torino, Italy and*

<sup>3</sup>*Departamento de Física, Universidad Nacional de La Plata,  
C. C. 67, 1900 La Plata, Argentina*

(Dated: June 14, 2021)

## Abstract

The non–mesonic weak decay of double– $\Lambda$  hypernuclei is studied within a microscopic diagrammatic approach. Besides the nucleon–induced mechanism,  $\Lambda N \rightarrow nN$ , widely studied in single– $\Lambda$  hypernuclei, additional hyperon–induced mechanisms,  $\Lambda\Lambda \rightarrow \Lambda n$ ,  $\Lambda\Lambda \rightarrow \Sigma^0 n$  and  $\Lambda\Lambda \rightarrow \Sigma^- p$ , are accessible in double– $\Lambda$  hypernuclei and are investigated here. As in previous works on single– $\Lambda$  hypernuclei, we adopt a nuclear matter formalism extended to finite nuclei via the local density approximation and a one–meson exchange weak transition potential (including the ground state pseudoscalar and vector octets mesons) supplemented by correlated and uncorrelated two–pion–exchange contributions. The weak decay rates are evaluated for hypernuclei in the region of the experimentally accessible light hypernuclei  ${}^{10}_{\Lambda\Lambda}\text{Be}$  and  ${}^{13}_{\Lambda\Lambda}\text{B}$ . Our predictions are compared with a few previous evaluations. The rate for the  $\Lambda\Lambda \rightarrow \Lambda n$  decay is dominated by  $K^-$ ,  $K^{*-}$  and  $\eta$ –exchange and turns out to be about 2.5% of the free  $\Lambda$  decay rate,  $\Gamma_{\Lambda}^{\text{free}}$ , while the total rate for the  $\Lambda\Lambda \rightarrow \Sigma^0 n$  and  $\Lambda\Lambda \rightarrow \Sigma^- p$  decays, dominated by  $\pi$ –exchange, amounts to about 0.25% of  $\Gamma_{\Lambda}^{\text{free}}$ . The experimental measurement of these decays would be essential for the beginning of a systematic study of the non–mesonic decay of strangeness  $-2$  hypernuclei. This field of research could also shed light on the possible existence and nature of the  $H$ –dibaryon.

## I. INTRODUCTION

Strangeness nuclear physics plays an important role in modern nuclear and hadronic physics and involves important connections with astrophysical processes and observables as well as with QCD. In particular, the weak decay of  $\Lambda$  hypernuclei is the only actual source of information on strangeness-changing four-baryon weak interactions. A great variety of theoretical and experimental studies were performed on the decay of such systems. Let us mention the experimental and theoretical analysis of nucleon-coincidence emission spectra and the theoretical modeling of the decay channels within complete one-meson-exchange weak transition potentials, which in some case have been supplemented by a two-pion-exchange mechanism. A reasonable agreement between data and predictions have been reached for the mesonic and non-mesonic decay rates, the  $\Gamma_n/\Gamma_p$  ratio between the neutron- and the proton-induced decay widths, the  $\Gamma_2/\Gamma_{\text{NM}}$  ratio between the two-nucleon induced and the total non-mesonic rates, and the intrinsic asymmetry parameter  $a_\Lambda$  for the decay of polarized hypernuclei [1]. Nevertheless, discrepancies between theory and experiment are still present for the emission spectra involving protons [2].

Despite their implications on the possible existence of dibaryon states and multi-strangeness hypernuclei and on the study of compact stars, much less is known on strangeness  $-2$  hypernuclei. Little information is available on cascade hypernuclei, for instance on the  $\Xi$ -nucleus potential. The existence of the strong  $\Xi^-p \rightarrow \Lambda\Lambda$  reaction makes  $\Xi$  Hypernuclei unstable with respect to the strong interaction. However, this conversion reaction can be exploited to produce double- $\Lambda$  hypernuclei.

Investigations on the structure of double- $\Lambda$  hypernuclei are important to determine the  $\Lambda\Lambda$  strong interaction, which is poorly known at present. Indeed, only a few double- $\Lambda$  hypernuclei events have been studied experimentally up to date. In KEK experiments,  ${}^4_{\Lambda\Lambda}\text{H}$ ,  ${}^6_{\Lambda\Lambda}\text{He}$  and  ${}^{10}_{\Lambda\Lambda}\text{Be}$  have been identified, while less unambiguous events were recorded for  ${}^6_{\Lambda\Lambda}\text{He}$  and  ${}^{10}_{\Lambda\Lambda}\text{Be}$  in the 60's and for  ${}^{13}_{\Lambda\Lambda}\text{B}$  in the early 90's [3]. The observation of the so-called NAGARA event implies a weak and attractive  $\Lambda\Lambda$  interaction, i.e., a bond energy  $\Delta B_{\Lambda\Lambda}({}^6_{\Lambda\Lambda}\text{He}) \equiv B_{\Lambda\Lambda}({}^6_{\Lambda\Lambda}\text{He}) - 2B_\Lambda({}^5_\Lambda\text{He}) = (0.67 \pm 0.17)$  MeV [4]. In Ref.[5] the authors demonstrated that this bond energy value, which will be employed in the present work as the binding energy between the two  $\Lambda$ 's, describes well double- $\Lambda$  hypernuclear data in the mass range from 6 to 13. Future experiments on strangeness  $-2$  hypernuclei will be carried

out at J-PARC [6] and FAIR (PANDA Collaboration) [7].

On the weak interaction side, double- $\Lambda$  hypernuclei offer the opportunity to access the following  $\Lambda$ -induced  $\Lambda$  decay channels:  $\Lambda\Lambda \rightarrow \Lambda n$ ,  $\Lambda\Lambda \rightarrow \Sigma^- p$ ,  $\Lambda\Lambda \rightarrow \Sigma^0 n$  (with a  $\Delta S = 1$  change in strangeness) and  $\Lambda\Lambda \rightarrow nn$  ( $\Delta S = 2$ ). The initial  $\Lambda\Lambda$  pair is coupled to  $S = 0$  and  $J = 0$ , thus only two non-mesonic decay channels are accessible:  $^1S_0 \rightarrow ^1S_0$  and  $^1S_0 \rightarrow ^3P_0$  in spectroscopic notation. No data is available on these decays, apart from the claim for the observation of a single event at KEK [8]. The experimental signature of a  $\Lambda\Lambda \rightarrow \Lambda n$  decay is clear, i.e., the emission of a large momentum  $\Lambda$  ( $\sim 425$  MeV), but the major problem is that these events are expected to be rather rare. The usual neutron- and proton-induced decays,  $\Lambda n \rightarrow nn$  and  $\Lambda p \rightarrow np$ , dominate over the  $\Lambda$ -induced ones in double- $\Lambda$  hypernuclei.

Realistic calculation and improved measurements of the  $\Lambda$ -induced  $\Lambda$  weak decays could also provide hints on the possible existence of the long-hunted  $H$ -dibaryon. A reliable calculation is important in the design of future experiments at J-PARC and FAIR, where these weak processes could be unambiguously observed for the first time.

Only a few predictions are available for such interesting strangeness-changing processes [9–11]; unfortunately, there are major disagreements among the predictions of these works, which adopted different frameworks. Their results are discussed in the following together with the new ones obtained here.

In this paper we present a microscopic calculation of both the  $\Lambda$ - and nucleon-induced  $\Lambda$  decay rates for double- $\Lambda$  hypernuclei by using a nuclear matter formalism (the  $\Lambda\Lambda \rightarrow nn$  decay channel is not considered here since, requiring a strangeness variation of 2 units, it is much less likely than the other  $\Lambda$ -induced processes); results for finite hypernuclei in the mass range of the empirically interesting  $^{10}_{\Lambda\Lambda}\text{Be}$  and  $^{13}_{\Lambda\Lambda}\text{B}$  systems are reported within the local density approximation. The same microscopic approach showed that Pauli exchange and ground state correlation contributions are very important for a detailed calculation of the rates, the asymmetry parameter and the nucleon emission spectra in the non-mesonic weak decay of  $\Lambda$  hypernuclei [2, 12–14]. Less pronounced effects have been reported by including the  $\Delta$ -baryon resonance in the microscopic approach [15].

The paper is organized as follows. In Section II we present the theoretical formalism employed for the evaluation of the decay rates. In Section III the numerical results are discussed and compared with previous calculations. Finally, in Section IV we draw our conclusions.

## II. FORMALISM

Let us start by writing the total non-mesonic decay rate for a double- $\Lambda$  hypernucleus as:

$$\Gamma_{\text{NM}} = \Gamma_{\text{N}} + \Gamma_{\Lambda}, \quad (1)$$

where:

$$\Gamma_{\text{N}} = \Gamma(\Lambda n \rightarrow nn) + \Gamma(\Lambda p \rightarrow np) \equiv \Gamma_n + \Gamma_p, \quad (2)$$

$$\begin{aligned} \Gamma_{\Lambda} &= \Gamma(\Lambda\Lambda \rightarrow \Lambda n) + \Gamma(\Lambda\Lambda \rightarrow \Sigma^0 n) + \Gamma(\Lambda\Lambda \rightarrow \Sigma^- p) \\ &\equiv \Gamma_{\Lambda n} + \Gamma_{\Sigma^0 n} + \Gamma_{\Sigma^- p}, \end{aligned} \quad (3)$$

are the total nucleon- and  $\Lambda$ -induced decay rates, respectively. The definitions of the partial rates  $\Gamma_n$ ,  $\Gamma_p$ ,  $\Gamma_{\Lambda n}$ ,  $\Gamma_{\Sigma^0 n}$  and  $\Gamma_{\Sigma^- p}$  are self-explanatory. We do not consider two-baryon induced decay mechanisms.

As in previous papers on  $\Lambda$  hypernuclei, we adopt a microscopic formalism. In this many-body technique the calculation is performed in infinite nuclear matter and then it is extended to finite nuclei through the local density approximation (LDA) [16].

The many-body contributions we consider for describing the  $\Lambda\Lambda \rightarrow YN$  processes in nuclear matter are given by the Goldstone diagrams of Fig.1. They provide the various decay widths through the relation  $\Gamma_f = -2 \text{Im} \Sigma_f^{\Lambda\Lambda}$ ,  $\Sigma_f^{\Lambda\Lambda}$  being the  $\Lambda\Lambda$  self-energy and  $f = \Lambda n, \Sigma^0 n$  and  $\Sigma^- p$  denoting the possible final states.

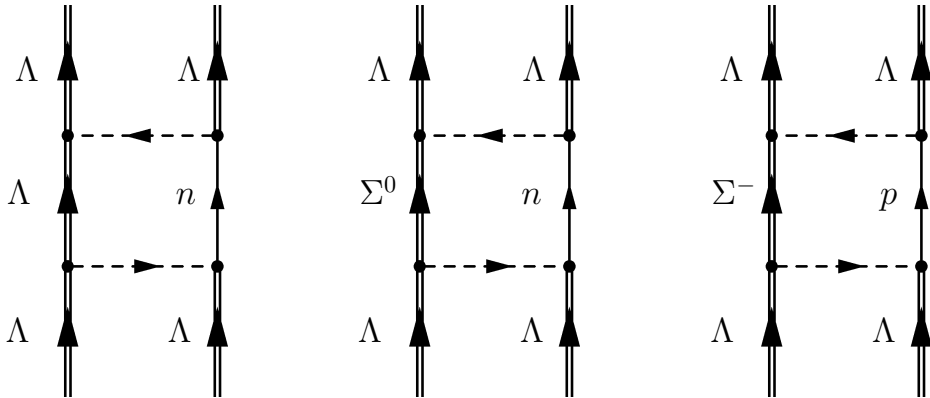


FIG. 1: Goldstone diagrams for the evaluation of the  $\Lambda\Lambda \rightarrow \Lambda n$ ,  $\Lambda\Lambda \rightarrow \Sigma^0 n$  and  $\Lambda\Lambda \rightarrow \Sigma^- p$  decay rates in infinite nuclear matter.

Let us consider infinite nuclear matter with Fermi momentum  $k_F$  and denote the four-momenta of the initial  $\Lambda$ 's with  $k = (k_0, \mathbf{k})$  and  $k' = (k'_0, \mathbf{k}')$  and the four-momenta of the final particles by  $p_1 = (p_{10}, \mathbf{p}_1)$  (hyperon) and  $p_2 = (p_{20}, \mathbf{p}_2)$  (nucleon). In a schematic way, for the Goldstone diagrams of Fig. 1 one obtains the partial decay width to the  $YN$  ( $= \Lambda n$ ,  $\Sigma^0 n$  and  $\Sigma^- p$ ) final state as follows:

$$\Gamma_{YN}(\mathbf{k}, k_F) = \sum_f |\langle f | V^{\Lambda\Lambda \rightarrow YN} | 0 \rangle_{k_F}|^2 \delta(E_f - E_0) , \quad (4)$$

where  $V^{\Lambda\Lambda \rightarrow YN}$  is the weak transition potential,  $|0\rangle_{k_F}$  denotes the initial state with energy  $E_0$  including the nuclear matter ground state and the two  $\Lambda$ 's in the  $1s$  level, and  $|f\rangle$  the possible final states with energy  $E_f$  including nuclear matter and the  $YN$  pair. Note also that momentum conservation, i.e.,  $\mathbf{k}' = \mathbf{p}_1 + \mathbf{p}_2 - \mathbf{k}$ , implies that only one of the initial momenta ( $\mathbf{k}$ ) is an independent variable once  $\mathbf{p}_1$  and  $\mathbf{p}_2$  are integrated out, as in Eq. (4).

The decay rates for a finite hypernucleus are obtained from the previous partial widths via the LDA:

$$\Gamma_{YN} = \int d\mathbf{k} |\tilde{\psi}_\Lambda(\mathbf{k})|^2 \int d\mathbf{r} |\psi_\Lambda(\mathbf{r})|^2 \Gamma_{YN}(\mathbf{k}, k_F(r)) . \quad (5)$$

This approximation (see also Appendix A) consists in introducing a local nucleon Fermi momentum  $k_F(r) = \{3\pi^2\rho(r)/2\}^{1/3}$  in terms of the density profile  $\rho(r)$  of the nuclear core and then in averaging the partial widths over the nuclear volume. This average is weighted by the probability per unit volume of finding the  $\Lambda$  which then transforms into the final nucleon at a given position  $\mathbf{r}$ ,  $|\psi_\Lambda(\mathbf{r})|^2$ . A further average is performed over the momentum distributions of the  $\Lambda$ ,  $\tilde{\psi}_\Lambda(\mathbf{k})$  (both initial  $\Lambda$ 's lies in the  $1s_{1/2}$  single-particle state). The calculation is performed for double- $\Lambda$  hypernuclei with mass number  $A = 10$ – $13$  in order to mimic the behavior of the experimentally accessible finite hypernuclei  $^{10}_{\Lambda\Lambda}\text{Be}$  and  $^{13}_{\Lambda\Lambda}\text{B}$ . As in Ref. [9], for the function  $\psi_\Lambda(\mathbf{r})$  we use a  $1s_{1/2}$  harmonic oscillator wave-function; its frequency  $\hbar\omega = 13.6$  MeV is obtained from the fit of Ref. [17] of the experimental binding energies of  $^6_{\Lambda\Lambda}\text{He}$ ,  $^{10}_{\Lambda\Lambda}\text{Be}$  and  $^{13}_{\Lambda\Lambda}\text{B}$ . The energies of the initial  $\Lambda$  with momentum  $\mathbf{k}$  is given by  $k_0 = m_\Lambda + \mathbf{k}^2/(2m_\Lambda) + V_\Lambda$ , where for the binding term we adopt the value  $V_\Lambda = -\hbar\omega = -13.6$  MeV.

Before we give explicit expressions for the decay widths in nuclear matter, it is convenient to show the general form of the weak transition potential. The standard weak, strangeness-

changing transition potential for the  $\Lambda\Lambda \rightarrow YN$  processes can be written as:

$$V^{\Lambda\Lambda \rightarrow YN}(q) = \sum_{\tau=0,1} \mathcal{O}_\tau V_\tau(q), \quad \mathcal{O}_\tau = \begin{cases} 1 & \text{for } \tau = 0 \\ \boldsymbol{\tau}_1 \cdot \boldsymbol{\tau}_2 & \text{for } \tau = 1 \end{cases}, \quad (6)$$

where

$$\begin{aligned} V_\tau(q) = (G_F m_\pi^2) \{ & S_\tau(q) \boldsymbol{\sigma}_1 \cdot \hat{\mathbf{q}} + S'_\tau(q) \boldsymbol{\sigma}_2 \cdot \hat{\mathbf{q}} + P_{L,\tau}(q) \boldsymbol{\sigma}_1 \cdot \hat{\mathbf{q}} \boldsymbol{\sigma}_2 \cdot \hat{\mathbf{q}} \\ & + P_{C,\tau}(q) + P_{T,\tau}(q) (\boldsymbol{\sigma}_1 \times \hat{\mathbf{q}}) \cdot (\boldsymbol{\sigma}_2 \times \hat{\mathbf{q}}) \\ & + i S_{V,\tau}(q) (\boldsymbol{\sigma}_1 \times \boldsymbol{\sigma}_2) \cdot \hat{\mathbf{q}} \}. \end{aligned} \quad (7)$$

The functions  $S_\tau(q)$ ,  $S'_\tau(q)$ ,  $P_{L,\tau}(q)$ ,  $P_{C,\tau}(q)$ ,  $P_{T,\tau}(q)$  and  $S_{V,\tau}(q)$  contain baryon–baryon short range correlations and vertex form factors and are taken from the Appendix B of Ref. [18], with the modifications concerning the baryon coupling constants discussed in the Appendix B of the present paper. The values  $\tau = 0, 1$  stand for the isoscalar and isovector parts of the interaction, respectively.

To enforce antisymmetrization, for each one of the contributions of Fig. 1 we also consider the corresponding exchange contribution. In Fig. 2 we give the direct and exchange diagrams for  $\Lambda\Lambda \rightarrow \Lambda n$ . Through the standard rules for Goldstone diagrams one writes down the

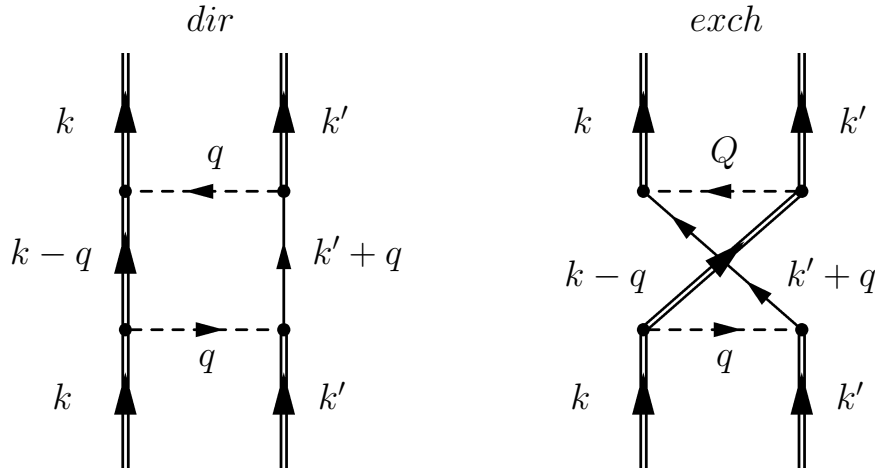


FIG. 2: Direct and exchange Goldstone diagrams for the  $\Lambda\Lambda \rightarrow \Lambda n$  decay.

explicit expression for these contributions. After performing the summations over spin and isospin together with the energy–integration one obtains the antisymmetrized decay rate:

$$\begin{aligned} \Gamma_{\Lambda n}(\mathbf{k}, k_F) = & \pi (G_F m_\pi^2)^2 \int \frac{d^3 p_1}{(2\pi)^3} \int \frac{d^3 p_2}{(2\pi)^3} (2 \mathcal{W}_0^{dir}(q) - \mathcal{W}_0^{exch}(q, Q)) \\ & \times \theta(|\mathbf{p}_2| - k_F) \delta(k_0 + k'_0 - E_\Lambda(p_1) - E_n(p_2)), \end{aligned}$$

where  $E_\Lambda$  ( $E_n$ ) is the total  $\Lambda$  (neutron) energy, while  $q = k - p_1$  and  $Q = p_2 - k$ . For the direct term, the momentum matrix–element of the interaction turns out to be:

$$\mathcal{W}_0^{dir}(q) = \{S_0^2(q) + S_0'^2(q) + P_{L,0}^2(q) + P_{C,0}^2(q) + 2P_{T,0}^2(q) + 2S_{V,0}^2(q)\}, \quad (8)$$

while for the exchange term we have:

$$\begin{aligned} \mathcal{W}_{exch}(q, Q) = & (\hat{\mathbf{q}} \cdot \hat{\mathbf{Q}})S_0(q, Q) + (2(\hat{\mathbf{q}} \cdot \hat{\mathbf{Q}})^2 - 1)P_{L,0}(q)P_{L,0}(Q) \\ & + 2((\hat{\mathbf{q}} \cdot \hat{\mathbf{Q}})^2 - 1)P_{T,0}(q)P_{T,0}(Q) \\ & - 2(\hat{\mathbf{q}} \cdot \hat{\mathbf{Q}})^2(P_{L,0}(q)P_{T,0}(Q) + P_{L,0}(Q)P_{T,0}(q)) \\ & + P_{C,0}(q)P_{C,0}(Q) + P_{C,0}(q)P_{L,0}(Q) + P_{C,0}(Q)P_{L,0}(q) \\ & + 2(P_{C,0}(q)P_{T,0}(Q) + P_{C,0}(Q)P_{T,0}(q)), \end{aligned} \quad (9)$$

where we have defined:

$$\begin{aligned} S_0(q, Q) = & (S_0(q) + S_0'(q))(S_0(Q) + S_0'(Q)) \\ & - 2(S_0(q)S_{V,0}(Q) + S_{V,0}(q)S_0(Q)) \\ & + 2(S_0'(q)S_{V,0}(Q) + S_{V,0}(q)S_0'(Q)). \end{aligned} \quad (10)$$

Note from Eqs. (8)–(10) that, being the  $\Lambda\Lambda \rightarrow \Lambda n$  weak potential of isoscalar nature, we have fixed  $\tau = 0$  in Eqs. (6) and (7). In Appendix B we present explicit expressions for the  $\Lambda\Lambda \rightarrow \Sigma^0 n$  and  $\Lambda\Lambda \rightarrow \Sigma^- p$  decay rates.

We assume the  $\Delta I = 1/2$  rule on the isospin change to be valid for all weak transition, although it is phenomenologically justified only for the  $\Lambda N \pi$  weak free vertex. Thus, by neglecting the small mass difference between  $\Sigma^0$  and  $\Sigma^-$  one simply obtains that the rates for decays into  $\Sigma^0 n$  and  $\Sigma^- p$  states are simply related by:

$$\frac{\Gamma_{\Sigma^- p}}{\Gamma_{\Sigma^0 n}} = 2, \quad (11)$$

and it is sufficient to calculate the decay rates  $\Gamma_{\Lambda n}$  and  $\Gamma_{\Sigma^0 n}$ .

We adopt a meson–exchange description of the weak transition potential including  $\pi$ ,  $\eta$ ,  $K$ ,  $\rho$ ,  $\omega$  and  $K^*$  mesons (these contribute to the one–meson–exchange part, denote by OME in the following) together with a two–pion–exchange mechanism (TPE). The latter has been obtained from the  $\Lambda N \rightarrow \Lambda N$  scalar–isoscalar two–pion–exchange strong interaction potential derived in Ref. [19] by a chiral unitary approach and consists in both an uncorrelated

and a correlated part. The present work is the first one to include the TPE mechanism. Since isospin is conserved in strong vertex, the  $\Lambda\Lambda \rightarrow \Lambda n$  decay process has isoscalar character and only the  $\eta$ ,  $K$ ,  $\omega$ ,  $K^*$  exchange and TPE contribute, while for  $\Lambda\Lambda \rightarrow \Sigma^0 n$  isoscalar transitions are prohibited and the contributing mesons are  $\pi$ ,  $K$ ,  $\rho$  and  $K^*$ . At the OME level one naively expects the  $\Lambda\Lambda \rightarrow \Lambda n$  decay ( $\Lambda\Lambda \rightarrow \Sigma^- p$ ,  $\Lambda\Lambda \rightarrow \Sigma^0 n$  decays) to be dominated by  $K$ -exchange ( $\pi$ -exchange). In particular, from the  $\Lambda\Lambda \rightarrow \Lambda n$  ( $\Lambda\Lambda \rightarrow \Sigma^0 n$ ) channel one could obtain information on the  $\Lambda\Lambda K$  ( $\Lambda\Sigma K$ ) vertex; these vertices are important to constrain  $SU(3)$  chiral perturbation theory [9].

Analyses of  $\Sigma$  formation spectra in the  $(K^-, \pi^\pm)$  and  $(\pi^+, K^+)$  reactions showed that the  $\Sigma$ -nucleus potential has a substantial isospin-dependence and, with the exception of very light systems (the only quasibound state of a  $\Sigma$  in a nucleus has been observed in  ${}^4_\Sigma\text{He}$ ), is repulsive:  $V_\Sigma \sim +(10 - 50)$  MeV at normal nuclear density. In the present calculation we adopt the value  $V_\Sigma = +30$  MeV.

### III. RESULTS

The calculations refer to the mass range corresponding to the experimentally accessible  ${}^{10}_{\Lambda\Lambda}\text{Be}$  and  ${}^{13}_{\Lambda\Lambda}\text{B}$  hypernuclei. Practically, the calculations are performed with  $A = N + Z + 2 = 12$  and an equal number of neutrons and protons,  $N = Z = 5$ . We verified that the numerical results does not change appreciably by changing  $A$  by one or two units: we will refer to them as the results for  $A \sim 12$  double- $\Lambda$  hypernuclei.

In Table I we give our results for the  $\Lambda\Lambda \rightarrow \Lambda n$ ,  $\Lambda\Lambda \rightarrow \Sigma^0 n$  and  $\Lambda\Lambda \rightarrow \Sigma^- p$  weak decay widths. Predictions are given for the individual meson exchanges and for the most relevant combinations among them. Note that the results for  $\Gamma_{\Sigma^- p}$  are obtained as  $\Gamma_{\Sigma^- p} = 2\Gamma_{\Sigma^0 n}$  since only  $\Delta I = 1/2$  transitions are considered here. As anticipated, the rate  $\Gamma_{\Lambda n}$  ( $\Gamma_{\Sigma^0 n}$ ) has no contribution from isovector (isoscalar) mesons.

In the OME sector the rate  $\Gamma_{\Lambda n}$  receives major contributions by  $K$ - and  $K^*$ -exchange. The  $\eta$  contribution is smaller but non-negligible. Instead, both the  $\omega$ -exchange and the TPE contributions are negligible; the TPE provides the smallest contribution. The addition of  $K$ - and  $K^*$ -exchange provides a decay rate which is about 65% larger than the complete result for  $\Gamma_{\Lambda n}$  because of a constructive interference between the two meson contributions. However, the further addition of the  $\eta$  meson, due to a destructive interference, lowers the

TABLE I: Results for the  $\Lambda\Lambda \rightarrow \Lambda n$ ,  $\Lambda\Lambda \rightarrow \Sigma^0 n$  and  $\Lambda\Lambda \rightarrow \Sigma^- p$  weak decay widths in  $A \sim 12$  double- $\Lambda$  hypernuclei are given as a percentage of the free  $\Lambda$  decay rate. Predictions are given for the individual contributing mesons and for the most relevant meson combinations.

Model and Ref.	$\Gamma_{\Lambda n}$	$\Gamma_{\Sigma^0 n}$	$\Gamma_{\Sigma^- p}$
$\pi$	–	0.070	0.140
$K$	1.73	0.001	0.002
$\eta$	0.35	–	–
$\rho$	–	0.001	0.002
$K^*$	0.84	0.002	0.004
$\omega$	0.01	–	–
TPE	0.002	–	–
$\pi + K + K^*$	4.14	0.081	0.162
$\pi + K + K^* + \eta$	2.57	0.081	0.162
All	2.48	0.084	0.168

decay rate to be only 4% larger than the complete result.

The rates  $\Gamma_{\Sigma^0 n}$  and  $\Gamma_{\Sigma^- p}$  are much smaller than  $\Gamma_{\Lambda n}$  and, as expected, are dominated by  $\pi$ -exchange. Much smaller single contributions originate from  $K^-$ ,  $K^{*-}$  and  $\rho$ -exchange. However, the combined effect of these mesons is to increase the rates by about 20% thanks to constructive interference effects. From the kinematics point of view, mesons heavier than the pion are expected to contribute less to the rates  $\Gamma_{\Sigma^0 n}$  and  $\Gamma_{\Sigma^- p}$  than to the rate  $\Gamma_{\Lambda n}$  since the  $\Lambda\Lambda \rightarrow \Lambda n$  process is characterized by larger momentum transfers than the  $\Lambda\Lambda \rightarrow \Sigma^0 n$  and  $\Lambda\Lambda \rightarrow \Sigma^- p$  processes. This is confirmed by the results of Table I: the  $\Gamma_{\Lambda n}$  rate receives substantial contributions from  $K^-$ ,  $K^{*-}$  and  $\eta$ -exchange, while  $\Gamma_{\Sigma^0 n}$  is dominated by  $\pi$ -exchange.

Before comparing the above predictions with those obtained in previous calculations, in Table II we present our results for the nucleon-induced non-mesonic decay rates together with determinations from Refs. [9, 10]. Our predictions for  $\Gamma_n$  and  $\Gamma_p$  in  $A \sim 12$  double- $\Lambda$  hypernuclei are larger than previously obtained for  ${}^6_{\Lambda\Lambda}\text{He}$ ; indeed, it is well established that, in single- $\Lambda$  hypernuclei, the values of the  $\Lambda N \rightarrow nN$  rates are increasing as a function

TABLE II: Predictions for the nucleon-induced non-mesonic weak decay rates for  $A \sim 12$  double- $\Lambda$  hypernuclei. The results of the present work are given together with previous ones available for  ${}^6_{\Lambda\Lambda}\text{He}$  [9, 10]. The decay rates are in units of the free  $\Lambda$  decay width.

Model and Ref.	$\Gamma_n$	$\Gamma_p$	$\Gamma_n/\Gamma_p$	$\Gamma_N = \Gamma_n + \Gamma_p$
This Work ( $A \sim 12$ )	0.48	1.12	0.43	1.60
OME ( ${}^6_{\Lambda\Lambda}\text{He}$ ) [9]	0.30	0.66	0.46	0.96
$\pi + 2\pi/\rho + 2\pi/\sigma$ ( ${}^6_{\Lambda\Lambda}\text{He}$ ) [10]	0.295	0.441	0.669	0.736

of  $A$  and saturate for  $A \sim 20$ . One expects the neutron- and proton-induced rates for a double- $\Lambda$  hypernucleus to be larger than twice the corresponding rates for a single- $\Lambda$  hypernucleus with one unit less mass number:  $\Gamma_N({}^A_{\Lambda\Lambda}Z) > 2\Gamma_N({}^{A-1}_\Lambda Z)$ . Apart from the fact that a double- $\Lambda$  hypernucleus has twice the number of  $\Lambda$ 's than a single- $\Lambda$  hypernucleus, one has to consider that the binding energy of a  $\Lambda$  is larger in  ${}^A_{\Lambda\Lambda}Z$  than in  ${}^{A-1}_\Lambda Z$ . This is well confirmed experimentally by binding data on  ${}^6_{\Lambda\Lambda}\text{He}$  and  ${}^5_\Lambda\text{He}$ . The same behavior is expected in our mass range [22], although for increasing  $A$  the  $\Lambda$  binding energies for double- $\Lambda$  and single- $\Lambda$  hypernuclei should converge towards a common value. Our results confirm the described behavior: the total nucleon-induced non-mesonic decay rate obtained for an  $A = 12$  double- $\Lambda$  hypernucleus,  $\Gamma_N = 1.60\Gamma_\Lambda^{\text{free}}$ , is about 5% larger than twice the same rate we obtain within the same framework and weak potential model for  ${}^{11}_\Lambda\text{B}$ ,  $\Gamma_N({}^{11}_\Lambda\text{B}) = 0.76\Gamma_\Lambda^{\text{free}}$ .

In Table III our final results for the  $\Lambda\Lambda \rightarrow \Lambda n$ ,  $\Lambda\Lambda \rightarrow \Sigma^0 n$  and  $\Lambda\Lambda \rightarrow \Sigma^- p$  decay rates in  $A \sim 12$  double- $\Lambda$  hypernuclei are given together with existing calculations for  ${}^6_{\Lambda\Lambda}\text{He}$  and  ${}^{10}_{\Lambda\Lambda}\text{Be}$  [9–11].

Our calculation is easily comparable with the finite nucleus (single-particle shell model) OME calculation of Ref. [9] since TPE turned out to give a negligible contribution in the present calculation and the OME models employed in both works have the same pseudoscalar and vector mesons content. Our predictions for  $\Gamma_{\Lambda n}$ ,  $\Gamma_{\Sigma^0 n}$  and  $\Gamma_{\Sigma^- p}$  are smaller, by 30–40%, than the ones of the finite nucleus calculation. We think this is mainly due to the fact that in Ref. [9] a lighter hypernucleus,  ${}^6_{\Lambda\Lambda}\text{He}$ , was considered. Indeed, we proved numerically that the  $\Lambda$ -induced  $\Lambda$  decay rate  $\Gamma_\Lambda = \Gamma_{\Lambda n} + \Gamma_{\Sigma^0 n} + \Gamma_{\Sigma^- p}$  decreases for increasing mass number  $A$ : a decrease of 2% in the rate  $\Gamma_{\Lambda n}$  is obtained if the calculation is performed with  $A = 10$  instead of  $A = 12$  (note that our LDA calculation cannot be extended to small mass

TABLE III: Predictions for the  $\Lambda\Lambda \rightarrow \Lambda n$ ,  $\Lambda\Lambda \rightarrow \Sigma^0 n$  and  $\Lambda\Lambda \rightarrow \Sigma^- p$  weak decay rates for  $A \sim 12$  double- $\Lambda$  hypernuclei of the present work and for  ${}^6_{\Lambda\Lambda}\text{He}$  and  ${}^{10}_{\Lambda\Lambda}\text{Be}$  from previous works. The decay rates are in units of  $10^{-2} \Gamma_{\Lambda}^{\text{free}}$ ,  $\Gamma_{\Lambda}^{\text{free}}$  being the free  $\Lambda$  decay width.

Model and Ref.	$\Gamma_{\Lambda n}$	$\Gamma_{\Sigma^0 n}$	$\Gamma_{\Sigma^- p}$
This Work ( $A \sim 12$ )	2.48	0.08	0.17
OME ( ${}^6_{\Lambda\Lambda}\text{He}$ ) [9]	3.6	0.13	0.26
$\pi + K + \omega + 2\pi/\rho + 2\pi/\sigma$ ( ${}^6_{\Lambda\Lambda}\text{He}$ ) [10]	5.3	0.10	0.20
$\pi + K + \omega + 2\pi/\rho + 2\pi/\sigma$ ( ${}^{10}_{\Lambda\Lambda}\text{Be}$ ) [10]	3.4	0.07	0.13
$\pi + K$ ( ${}^6_{\Lambda\Lambda}\text{He}$ ) [11]	0.03	0.51	1.00
$\pi + K + \text{DQ}$ ( ${}^6_{\Lambda\Lambda}\text{He}$ ) [11]	0.24	0.65	0.85

numbers as  $A = 6$ ). The results of Ref. [10] of Table III also corroborates this behavior. Note instead that the nucleon-induced  $\Lambda$  decay rate  $\Gamma_N = \Gamma_n + \Gamma_p$  (for both single- and double- $\Lambda$  hypernuclei) increases for increasing  $A$ . The different behavior of  $\Gamma_N$  and  $\Gamma_{\Lambda}$  as a function of  $A$  is easily explained as follows. On the one hand, the rate  $\Gamma_N$  increases and then saturates with  $A$  since it somehow measures the number of nucleons which can interact with the  $\Lambda$ , i.e., the nucleons which can induce a  $\Lambda N \rightarrow nN$  decay. On the other hand, for increasing  $A$  the average distance between two  $\Lambda$ 's in a double- $\Lambda$  hypernucleus increases and thus the rate  $\Gamma_{\Lambda}$  decreases. Our  $\Lambda$ -induced predictions exhibit a similar behavior of the ones of Ref. [9], which also enforced the  $\Delta I = 1/2$  rule: the ratio  $\Gamma_{\Lambda n}/\Gamma_{\Sigma^0 n}$  is about 28 in the finite nucleus approach, while in the present work:

$$\frac{\Gamma_{\Lambda n}}{\Gamma_{\Sigma^0 n}} \sim 30. \quad (12)$$

Another ratio between decay rates deserves to be considered: it involves the neutron-induced rate  $\Gamma_n$  and the  $\Lambda$ -induced rate  $\Gamma_{\Lambda n}$ . One expect the  $\Gamma_n/\Gamma_{\Lambda n}$  ratio to be driven by the number of  $\Lambda n$  pairs in the hypernucleus, i.e., by the number of neutrons  $N_n$  that can induce the non-mesonic decay. In a naive picture,  $\Gamma_n/\Gamma_{\Lambda n}$  is proportional to  $N_n$ . We obtain:

$$\frac{\Gamma_n}{\Gamma_{\Lambda n}} \sim 19.4, \quad (13)$$

while in the finite nucleus approach of Ref. [9]  $\Gamma_n/\Gamma_{\Lambda n} \sim 8.3$ . The different results are mainly due to the different neutron numbers in the two calculations,  $N_n = 5$  in the present

calculation and  $N_n = 2$  in Ref. [9]: indeed,  $(\Gamma_n/\Gamma_{\Lambda n})_{N_n=5}/(\Gamma_n/\Gamma_{\Lambda n})_{N_n=2} \sim 2.3$ , while the corresponding ratio between the neutron numbers is  $5/2 = 2.5$ .

In Ref. [10], a phenomenological, correlated two-pion-exchange ( $2\pi/\sigma + 2\pi/\rho$ ) mechanism was added to a  $\pi + K + \omega$ -exchange model for a finite nucleus calculation for  ${}^6_{\Lambda\Lambda}\text{He}$  and  ${}^{10}_{\Lambda\Lambda}\text{Be}$ . The authors found an improvement in the calculation of the  $\Gamma_n/\Gamma_p$  ratio for single- $\Lambda$  hypernuclei by including the  $2\pi/\sigma$  and  $2\pi/\rho$  potentials [20] together with  $K$ -exchange [10]. We note that in Ref. [10] the same  $\Lambda$  wave function previously adopted for  ${}^5_{\Lambda}\text{He}$  was used for  ${}^6_{\Lambda\Lambda}\text{He}$ , despite, as explained above, a  $\Lambda$  is more bound in  ${}^6_{\Lambda\Lambda}\text{He}$  than in  ${}^5_{\Lambda}\text{He}$ . This assumption leads to an underestimation of the  $\Gamma_n$  and  $\Gamma_p$  decay rates reported in Table II for  ${}^6_{\Lambda\Lambda}\text{He}$ . Concerning double- $\Lambda$  hypernuclei, in the same paper the wave function of  ${}^6_{\Lambda\Lambda}\text{He}$  ( ${}^{10}_{\Lambda\Lambda}\text{Be}$ ) was described by an  $\alpha + \Lambda + \Lambda$  three-body cluster model ( $\alpha + \alpha + \Lambda + \Lambda$  four-body cluster model). Although the final results for  ${}^{10}_{\Lambda\Lambda}\text{Be}$  are not very different from ours, a dominant contribution from  $2\pi/\sigma$ -exchange to the  $\Lambda\Lambda \rightarrow \Lambda n$  decay rate is obtained; this behavior is not confirmed by the chiral unitary approach based TPE mechanism adopted in the present study. The lack of details from Ref. [10] does not allow us to understand the origin of such a discrepancy. The ratio  $\Gamma_{\Lambda n}/\Gamma_{\Sigma^0 n}$  is about 53 (49) for  ${}^6_{\Lambda\Lambda}\text{He}$  ( ${}^{10}_{\Lambda\Lambda}\text{Be}$ ); both results are larger by about 80% than what found in the present paper and in Ref. [9]. Furthermore, the ratio  $\Gamma_n/\Gamma_{\Lambda n}$  is about 5.6 for  ${}^6_{\Lambda\Lambda}\text{He}$ , i.e., about 30% less than found in the finite nucleus calculation of Ref. [9] for the same hypernucleus.

In Ref. [11] an hybrid quark-meson approach is instead adopted, which includes  $\pi$ - and  $K$ -exchange at long and medium distances and a direct quark mechanism (basically, a valence quark picture of baryons based on an effective four-quark weak Hamiltonian) to account for the short-range part of the processes. The direct quark mechanism provides a large contribution to the  $\Gamma_{\Lambda n}$ ,  $\Gamma_{\Sigma^0 n}$  and  $\Gamma_{\Sigma^- p}$  decay rates and strongly violates the isospin rule (11) (see the results in Table III). We note that the  $\pi + K$  calculation provides  $\Gamma_{\Lambda n}^K/\Gamma_{\Sigma^0 n}^\pi = 0.06$ , in strong disagreement with the other calculations of Table III. We note that a simple evaluation in terms of the weak and strong coupling constants involved in the  $\Lambda\Lambda \rightarrow \Lambda n$  decay mediated by the  $K$  meson and the  $\Lambda\Lambda \rightarrow \Sigma^0 n$  decay mediated by the  $\pi$  meson indicates that the ratio  $\Gamma_{\Lambda n}^K/\Gamma_{\Sigma^0 n}^\pi$  (which is a good approximation of the ratio  $\Gamma_{\Lambda n}/\Gamma_{\Sigma^0 n}$ ; see the results of Table I) has to be larger than 1. When compared with the results of the present paper and of Ref. [9], the very small value of  $\Gamma_{\Lambda n}^K/\Gamma_{\Sigma^0 n}^\pi$  originates from a ‘very small’  $K$ -exchange (‘large’  $\pi$ -exchange) contribution to the  $\Lambda\Lambda \rightarrow \Lambda n$  ( $\Lambda\Lambda \rightarrow \Sigma^0 n$ ) channel. We point

out the strong disagreement concerning  $K$ -exchange:  $\Gamma_{\Lambda n}^K/(10^{-2}\Gamma_{\Lambda}^{\text{free}})$  is 0.03 in the hybrid quark-meson approach, while it is 1.7 (2.7) in the present approach (in the finite nucleus calculation of Ref. [9]). For the complete calculation, the hybrid quark-meson approach provides  $\Gamma_{\Lambda n}/\Gamma_{\Sigma^0 n} \sim 0.37$ .

As mentioned, no data is available on  $\Lambda$ -induced  $\Lambda$  decays, apart from the claim [8] for the observation of a single event in the KEK hybrid-emulsion experiment which led to the observation of the so-called NAGARA event concerning the observation of the  ${}^6_{\Lambda\Lambda}\text{He}$  hypernucleus. The authors interpreted this event as a weak decay of an unknown strangeness  $-2$  system into a  $\Sigma^- p$  pair. This result is difficult to interpret since the KEK experimental branching ratio (BR) for this process is of the order of  $10^{-2}$  while for the  $\Lambda\Lambda \rightarrow \Sigma^- p$  decay in a double- $\Lambda$  hypernucleus the BR is evaluated to be of the order of  $10^{-3}$  in the present work as well as in the previous determinations of Refs. [9, 10]. As done in Ref. [8], one could also speculate that the observed event corresponds to a decay of an  $H$ -dibaryon. As far as we know, there is only a dated calculation [21] concerning the  $H \rightarrow \Sigma^- p$  process, which, adapted to the case of a double- $\Lambda$  hypernucleus, provides a BR of the order of  $10^{-2}$ . Future measurements will be essential not only to establish the  $\Lambda$ -induced  $\Lambda$  weak decays studied here but also in order to clarify the question of the existence and nature of the  $H$ -dibaryon and eventually to establish its role in defining the properties of double- $\Lambda$  hypernuclei.

#### IV. CONCLUSIONS

A microscopic diagrammatic approach is used to evaluate the nucleon- and  $\Lambda$ -induced  $\Lambda$  decay in double- $\Lambda$  hypernuclei. The calculation is performed in nuclear matter and then extended to finite hypernuclei with mass numbers  $A \sim 12$  ( ${}^{10}_{\Lambda\Lambda}\text{Be}$  and  ${}^{13}_{\Lambda\Lambda}\text{B}$  are experimentally accessible cases) by means of the local density approximation. The present approach is the first one which takes into account the full one-meson-exchange weak transition potential together with a two-pion-exchange contribution. The one-meson-exchange potential contains the mesons of the ground state pseudoscalar and vector octets, while the two-pion-exchange potential includes correlated and uncorrelated contributions and is obtained from the chiral unitary approach of Ref. [19]. Such a complete potential model proved to be of crucial importance in consistently explaining the whole set of decay data on single- $\Lambda$  hypernuclei [1].

We confirm that the neutron- and proton-induced decay rates for the hypernucleus  ${}^A_{\Lambda\Lambda}Z$  with  $A \sim 12$  turn out to be larger (by about 5%) than twice the corresponding rates for the single- $\Lambda$  hypernucleus  ${}^{A-1}_\Lambda Z$ ; data indicates that the binding energy of a  $\Lambda$  is indeed larger in  ${}^A_{\Lambda\Lambda}Z$  than in  ${}^{A-1}_\Lambda Z$ .

The two-pion-exchange mechanism turns out to provide a negligible contribution to the  $\Lambda\Lambda \rightarrow \Lambda n$  non-mesonic decay of double- $\Lambda$  hypernucleus. The rate  $\Gamma_{\Lambda n}$  receives the major contributions from  $K$ - and  $K^*$ -exchange (however, the  $\eta$  meson cannot be neglected). The rates  $\Gamma_{\Sigma^0 n}$  and  $\Gamma_{\Sigma^- p}$ , which are much smaller than  $\Gamma_{\Lambda n}$  ( $\Gamma_{\Lambda n}/\Gamma_{\Sigma^0 n} = 29$  and  $\Gamma_{\Sigma^- p}/\Gamma_{\Sigma^0 n} = 2$  in virtue of the  $\Delta I = 1/2$  isospin rule), are dominated by  $\pi$ -exchange.

The total  $\Lambda$ -induced decay rate,  $\Gamma_\Lambda = \Gamma_{\Lambda n} + \Gamma_{\Sigma^0 n} + \Gamma_{\Sigma^- p}$ , amounts to about 1.7% of the total non-mesonic rate,  $\Gamma_{\text{NM}} = \Gamma_n + \Gamma_p + \Gamma_\Lambda$ . We also find that the rate  $\Gamma_\Lambda$  decreases as the hypernuclear mass number  $A$  increases since the average distance between two  $\Lambda$  in a double- $\Lambda$  hypernucleus is an increasing function of  $A$ .

Our final results for  $\Gamma_{\Lambda n}$ ,  $\Gamma_{\Sigma^0 n}$  and  $\Gamma_{\Sigma^- p}$  are in fairly good agreement with the ones of Refs. [9, 10] and in strong disagreement with those of Ref. [11].

We hope the present work may contribute to the start of a systematic investigation on the non-mesonic weak decays of double- $\Lambda$  hypernuclei. No reliable experimental evidence of interesting processes such as  $\Lambda\Lambda \rightarrow \Lambda n$ ,  $\Lambda\Lambda \rightarrow \Sigma^0 n$  and  $\Lambda\Lambda \rightarrow \Sigma^- p$  is available at present. Future measurements will also be essential to clarify the question of the existence and nature of the  $H$ -dibaryon and eventually to establish its interplay and/or mixing with the  $\Lambda\Lambda$  pair in determining the structure and weak decays properties of double- $\Lambda$  hypernuclei. New experimental programs at J-PARC and FAIR should thus be strongly supported.

## Appendix A

We present here the formal derivation of Eq. (5) which is used to calculate the decay rates in the local density approximation (LDA). Let us start by introducing the  $\Lambda$  pair wave function in coordinate space,  $\psi_{\Lambda\Lambda}(\mathbf{r}, \mathbf{r}')$ . In a double- $\Lambda$  hypernucleus both hyperons are paired in the lowest energy single-particle state  $1s$ . In the independent-particle approximation,  $\psi_{\Lambda\Lambda}(\mathbf{r}, \mathbf{r}')$  is simply factorized in terms of the individual  $\Lambda$  wave functions  $\psi_\Lambda(\mathbf{r})$  and  $\psi_\Lambda(\mathbf{r}')$  associated to the same energy eigenvalue:

$$\psi_{\Lambda\Lambda}(\mathbf{r}, \mathbf{r}') = \psi_\Lambda(\mathbf{r})\psi_\Lambda(\mathbf{r}') . \quad (\text{A1})$$

Let us denote with  $\mathbf{k}$  and  $\mathbf{k}'$  ( $\mathbf{p}_1$  and  $\mathbf{p}_2$ ) the momenta of the initial  $\Lambda$ 's (final hyperon and nucleon) for the  $\Lambda\Lambda \rightarrow YN$  decay. In the LDA one introduces the following rate for such a decay:

$$\Gamma_{YN}(\mathbf{k}) = \int d\mathbf{r} \int d\mathbf{r}' |\psi_{\Lambda\Lambda}(\mathbf{r}, \mathbf{r}')|^2 \Gamma_{YN}(\mathbf{k}, \mathbf{r}, \mathbf{r}') , \quad (\text{A2})$$

$\mathbf{k}$  being the momentum of one of the initial  $\Lambda$ 's. The final momenta  $\mathbf{p}_1$  and  $\mathbf{p}_2$  are integrated out to obtain  $\Gamma_{YN}(\mathbf{k}, \mathbf{r}, \mathbf{r}')$ . Note also that momentum conservation, i.e.,  $\mathbf{k}' = \mathbf{p}_1 + \mathbf{p}_2 - \mathbf{k}$ , implies that only one of the initial momenta ( $\mathbf{k}$ ) is an independent variable once  $\mathbf{p}_1$  and  $\mathbf{p}_2$  are integrated out. This is the reason why the integrand in Eq. (A2) is independent of  $\mathbf{k}'$ .

The rates for finite hypernuclei are thus obtained through the relation:

$$\Gamma_{YN} = \int d\mathbf{k} |\tilde{\psi}_{\Lambda}(\mathbf{k})|^2 \Gamma_{YN}(\mathbf{k}) , \quad (\text{A3})$$

$\tilde{\psi}_{\Lambda}(\mathbf{p})$  denoting the Fourier transform of  $\psi_{\Lambda}(\mathbf{r})$ .

Let us denote with  $\mathbf{r}$  the spatial point in which the final nucleon is created and with  $\mathbf{r}'$  the spatial point in which the initial  $\Lambda$  converts into the final  $\Lambda$ . Then, introduce a local nucleon Fermi momentum depending on the position in which the final nucleon is created,  $k_F(r) = \{3\pi^2\rho(r)/2\}^{1/3}$ ,  $\rho(r)$  being the density profile of the nuclear core. It follows that the function  $\Gamma_{YN}(\mathbf{k}, \mathbf{r}, \mathbf{r}')$  is independent of  $\mathbf{r}'$  and can be written as  $\Gamma_{YN}(\mathbf{k}, k_F(r))$ . Finally, from Eqs. (A1)–(A3) one simply obtains Eq. (5), which formally is the same relation used for the  $\Lambda N \rightarrow nN$  non-mesonic decays.

## Appendix B

Before presenting expressions for the evaluation of  $\Gamma_{\Sigma^0 n}$  and  $\Gamma_{\Sigma^- p}$ , we call attention to some changes in the baryon coupling constants with respect to our previous work. As mentioned, the expressions for the functions  $S_{\tau}(q)$ ,  $S'_{\tau}(q)$ ,  $P_{L,\tau}(q)$ ,  $P_{C,\tau}(q)$ ,  $P_{T,\tau}(q)$  and  $S_{V,\tau}(q)$  appearing in the weak transition potential  $V^{\Lambda\Lambda \rightarrow YN}$  of Eqs. (6) and (7) are given in Appendix B of Ref. [18], where they refer to the  $V^{\Lambda N \rightarrow NN}$  potential.

The  $V^{\Lambda\Lambda \rightarrow \Lambda n}$  transition potential, which is isoscalar, is obtained by fixing  $\tau = 0$  in Eqs. (6) and (7) and by making the following replacements for the strong coupling constants:  $g_{NN\eta} \rightarrow g_{\Lambda\Lambda\eta}$ ,  $g_{NN\omega}^V \rightarrow g_{\Lambda\Lambda\omega}^V$ ,  $g_{NN\omega}^T \rightarrow g_{\Lambda\Lambda\omega}^T$ . Analogously, the  $NNK$  and  $NNK^*$  weak parity conserving (PC) and parity violating (PV) coupling constants are replaced by the  $\Lambda\Lambda K$  and  $\Lambda\Lambda K^*$  couplings, respectively. The two-pion-exchange weak potential has

been obtained from the  $\Lambda N \rightarrow \Lambda N$  scalar–isoscalar two–pion–exchange strong interaction potential (including correlated and uncorrelated contributions) derived in Ref. [19] by a chiral unitary approach. This is obtained by replacing the  $g_{\pi NN}$  strong coupling constant by the weak parity–conserving coupling  $B_\pi = -7.15$  associated to the experimentally accessible  $\Lambda N\pi$  vertex.

For the  $V^{\Lambda\Lambda \rightarrow \Sigma^0 n}$  transition potential, which is isovector, we instead fix  $\tau = 1$  in Eqs. (6) and (7). The relevant coupling constants are obtained from the  $V^{\Lambda N \rightarrow NN}$  ones by the following replacements. For the strong coupling constants:  $g_{NN\pi} \rightarrow g_{\Lambda\Sigma\pi}$ ,  $g_{NN\rho}^V \rightarrow g_{\Lambda\Sigma\rho}^V$  and  $g_{NN\rho}^T \rightarrow g_{\Lambda\Sigma\rho}^T$ , while for the weak coupling constants:  $C_{NNK}^{PC} \rightarrow C_{\Lambda\Sigma K}^{PC}$ ,  $C_{NNK}^{PV} \rightarrow C_{\Lambda\Sigma K}^{PV}$ ,  $C_{NNK^*}^{PC} \rightarrow C_{\Lambda\Sigma K^*}^{PC}$  and  $C_{NNK^*}^{PV} \rightarrow C_{\Lambda\Sigma K^*}^{PV}$ .

As explained in the text, by neglecting the small mass difference between the hyperons  $\Sigma^0$  and  $\Sigma^-$ , isospin considerations lead to  $\Gamma_{\Sigma^- p} = 2\Gamma_{\Sigma^0 n}$ .

After performing the summations over spin and isospin together with the energy–integration one obtains the antisymmetrized  $\Lambda\Lambda \rightarrow \Sigma^0 n$  decay rate in nuclear matter as:

$$\Gamma_{\Sigma^0 n}(\mathbf{k}, k_F) = \frac{\pi}{3} (G_F m_\pi^2)^2 \int \frac{d^3 p_1}{(2\pi)^3} \int \frac{d^3 p_2}{(2\pi)^3} (2\mathcal{W}_1^{dir}(q) - \mathcal{W}^{exch}(q, Q)) \times \theta(|\mathbf{p}_2| - k_F) \delta(k_0 + k'_0 - E_{\Sigma^0}(p_1) - E_n(p_2)),$$

where  $E_\Lambda$  ( $E_n$ ) is the total  $\Lambda$  (neutron) energy. For the direct and exchange terms, the momentum matrix–element of the interaction turn out to be:

$$\mathcal{W}_1^{dir}(q) = \{S_1^2(q) + S_1'^2(q) + P_{L,1}^2(q) + P_{C,1}^2(q) + 2P_{T,1}^2(q) + 2S_{V,1}^2(q)\}, \quad (\text{B1})$$

and

$$\begin{aligned} \mathcal{W}^{exch}(q, Q) = & (\hat{\mathbf{q}} \cdot \hat{\mathbf{Q}})S_1(q, Q) + (2(\hat{\mathbf{q}} \cdot \hat{\mathbf{Q}})^2 - 1)P_{L,1}(q)P_{L,1}(Q) \\ & + 2((\hat{\mathbf{q}} \cdot \hat{\mathbf{Q}})^2 - 1)P_{T,1}(q)P_{T,1}(Q) \\ & - 2(\hat{\mathbf{q}} \cdot \hat{\mathbf{Q}})^2(P_{L,1}(q)P_{T,1}(Q) + P_{L,1}(Q)P_{T,1}(q)) \\ & + P_{C,1}(q)P_{C,1}(Q) + P_{C,1}(q)P_{L,1}(Q) + P_{C,1}(Q)P_{L,1}(q) \\ & + 2(P_{C,1}(q)P_{T,1}(Q) + P_{C,1}(Q)P_{T,1}(q)), \end{aligned} \quad (\text{B2})$$

respectively, where  $Q = q + k' - k$  and:

$$\begin{aligned} S_1(q, Q) = & (S_1(q) + S_1'(q))(S_1(Q) + S_1'(Q)) \\ & - 2(S_1(q)S_{V,1}(Q) + S_{V,1}(q)S_1(Q)) \\ & + 2(S_1'(q)S_{V,1}(Q) + S_{V,1}(q)S_1'(Q)). \end{aligned} \quad (\text{B3})$$

The finite hypernucleus decay rate  $\Gamma_{\Sigma^0 n}$  is then obtained by means of the LDA of Eq. (5).

### Acknowledgements

We would like to thank A. Ramos and A. Parreño for fruitful discussions. This work was partially supported by the CONICET, Argentina, under contract PIP 0032 and by the Agencia Nacional de Promociones Científicas y Técnicas, Argentina, under contract PICT-2010-2688,

- 
- [1] E. Botta, T. Bressani and G. Garbarino, *Eur. Phys. J. A* **48** (2012) 41; H. Ota, in *Hadron Physics* (IOS Press, Amsterdam, 2005). *Proc. of the International School of Physics 'E. Fermi' Course CLVIII*, edited by T. Bressani, A. Filippi and U. Wiedner, p. 21; W.M. Alberico and G. Garbarino, *Phys. Rep.* **369** (2002) 1.
  - [2] E. Bauer and G. Garbarino, *Phys. Lett. B* **698** (2011) 306.
  - [3] K. Nakazawa and H. Takahashi, *Prog. Theor. Phys. Suppl.* **185** (2010) 335.
  - [4] J. K. Ahn *et al.*, *Phys. Rev. C* **88** (2013) 014003; H. Takahashi *et al.* *Phys. Rev. Lett.* **87** (2001) 212502.
  - [5] A. Gal and D.J. Millener, *Phys. Lett. B* **701** (2011) 342; *Hyperfine Interact.* **210** (2012) 77.
  - [6] T. Takahashi, *Nucl. Phys. A* **914** (2013) 530.
  - [7] A. Sanchez Lorente *et al.*, *Hyperfine Interact.* **229** (2014) 45; U. Wiedner, *Prog. Part. Nucl. Phys.* **66** (2011) 477.
  - [8] T. Watanabe *et al.*, *Eur. Phys. J. A* **33** (2007) 265.
  - [9] A. Parreño, A. Ramos and C. Bennhold, *Phys. Rev. C* **65** (2001) 015205.
  - [10] K. Itonaga, T. Ueda and T. Motoba, *Nucl. Phys. A* **691** (2001) 197c. *Mod. Phys. Lett. A* **18** (2003) 135;
  - [11] K. Sasaki, T. Inoue and M. Oka, *Nucl. Phys. A* **726** (2003) 349.
  - [12] E. Bauer and G. Garbarino, *Nucl. Phys. A* **828** (2009) 29.
  - [13] E. Bauer and G. Garbarino, *Phys. Rev. C* **81** (2010) 064315.
  - [14] E. Bauer, G. Garbarino, A. Parreño and A. Ramos, *Phys. Rev. C* **85** (2012) 024321.
  - [15] E. Bauer and G. Garbarino, *Phys. Lett. B* **716** (2012) 249.

- [16] E. Oset and L. L. Salcedo, Nucl. Phys. **A 443**, 704 (1985).
- [17] J. Caro, C. Garcia-Recio and J. Nieves, Nucl. Phys. **A 646** (1999) 299.
- [18] E. Bauer and F. Krmpotić, Nucl. Phys. **A 717** (2003) 217.
- [19] K. Sasaki, E. Oset, and M.J. Vicente Vacas, Phys. Rev. **C 74** (2006) 064002; K. Sasaki, E. Oset and M. J. Vicente Vacas, Eur. Phys. J. **A 31** (2007) 557.
- [20] K. Itonaga, T. Ueda and T. Motoba, Phys. Rev. **C 65** (2002) 034617.
- [21] J. F. Donoghue, E. Golowich and B. R. Holstein, Phys. Rev. **D 34** (1986) 3434.
- [22] Note that available experimental values of the harmonic oscillator parameter  $\hbar\omega$  (obtained as the energy separation between the  $s$  and  $p$   $\Lambda$ -levels) are  $-10.8$  MeV for  ${}_{\Lambda}^{12}\text{C}$  and  $-13.6$  MeV for  $A = 6-13$  double- $\Lambda$  hypernuclei.